Original Study

Open Access

Bilel Boualleg*, Nadjet Bouacha

Analysis of the behavior of structures under the effect of progressive rupture of a cavity

https://doi.org/10.2478/sgem-2024-0019
received November 22, 2023; accepted July 15, 2024.

Abstract: The ground movements related to the presence of old underground cavities are often damaging to structures and infrastructures. Considering these ground movements in calculations will prevent considerable human loss and material damage. Many areas, both in Algeria and in abroad, are prone to instability caused by ground rupture and the phenomenon of sinkhole progression. The objectives of this work are first to numerically simulate the process of cavity collapse and second to analyze the impact of cavity properties on structure stability. A finite element model was established to analyze the influence of several cavity parameters (dimensions, volume, and spacing). Validation of the model relied on comparing numerical results with experimental data from scientific research, as well as those from analytical approaches. Adequate correlation was achieved. The study allowed deriving mathematical equations relating to several parameters, including cavity dimensions and position in the soil, soil characteristics, and footing width. These results will be considered to reduce the risk of surface structure instability.

Keywords: Soil-structure interaction; cavity; structure; modeling; rupture; footing; displacement.

1 Introduction

The frequent presence of underground cavities in certain developable areas poses a potential collapse risk that can be detrimental to the proper functioning of infrastructures and the safety of their users. Various studies have been conducted to investigate the issues caused by the collapse of underground cavities and the impact of these collapses on surface structures.

Table 1 summarizes the main research studies analyzing cavity collapse using experimental and numerical methods, classified chronologically.

Our work focuses on analyzing the interaction between the soil and the structure, first examining the progressive collapse of an underground cavity beneath a structure and then evaluating its impact on the stability of the structure. Finally, we conduct a parametric study to understand how cavity volume, depth, and spacing influence the stability of the structure.

To predict ground movements caused by cavity degradation, geotechnical engineers have various methods at their disposal. These methods include empirical approaches using detailed field data, analytical methods based on mechanical equations, and numerical methods. These approaches are documented in the scientific literature notably by Deck et al. (2006) and Dolzhenko (2002).

The main objectives of this study are to minimize the consequences of cavity collapse, maintain the stability of the structure, and reduce deformations observed at the structural elements level. Our methodological approach involved initially validating a numerical model, followed by calculating the collapse values using an analytical method. Test results were presented using a scaled-down model. In practice, empirical methods are often guided by analytical approaches or finite element calculations. These methods are then adjusted based on experimental curves, as highlighted by Aftes (1982).

The empirical approaches described by Peck (1969) for vertical displacements and by Lake et al. (1992) for horizontal displacements are used to predict ground surface movements after the excavation of a circular tunnel (see Figure 1). Equations 1 and 2 express vertical and horizontal displacements, respectively:

$$\text{Vertical displacement: } S(x) = S_{max} \times e^{-x^2/2i^2} \quad (1)$$

***Corresponding author: Bilel Boualleg,** Department of Civil Engineering, University of Souk-Ahras, BP 1553, 41000 Souk-Ahras, Algeria Laboratory of Management, Maintenance and Rehabilitation of Urban Equipment and Infrastructure (InfraRES), E-mail: b.bouallag@univ-soukahras.dz; http://orcid.org/0000-0002-3594-1914
Nadjet Bouacha, Department of Civil Engineering, University of Souk-Ahras, BP 1553, 41000 Souk-Ahras, Algeria Laboratory of Management, Maintenance and Rehabilitation of Urban Equipment and Infrastructure (InfraRES); http://orcid.org/0000-0001-2345-6789

Open Access. © 2024 Bilel Boualleg, Nadjet Bouacha, published by Sciendo. This work is licensed under the Creative Commons Attribution alone 4.0 License.

Table 1: Summary of conducted research studie.

Author	Year	Objective	Type
Nakai et al.	1997	Investigate the effect of 3D and expansion on ground movements during tunnel excavation	Experimental
Dyne	1998	Analyze the different parameters: the opening of the cavity, the width of the cavity, and the height of the covering	Experimental 2D scale model
Burd et al.	2000	Study soil-structure interaction during tunneling under masonry structures and analysis	Numerical MEF-OXFEM
Laefer	2001	Study the damage to structures on shallow foundations subject to soil movements induced by excavation	Experimental (a small-scale model of 1/10th).
Mahamma	2002	Study the soil-structure interaction phenomena during the collapse of a mine gallery. The collapse of the mine gallery was modeled by successive sinking of a cylinder along the axis of propagation of the rupture	Experimental
Shanin et al.	2004	The study of the effect of ground movements and their mechanical behavior during tunnel excavation.	Experimental trap model
Boumalla	2005	Vary a number of parameters such as the opening of the cavity, the height of the cover, the rate of initiation of a melt, or the subsidence of the ground	Experimental
Sung et al.	2006	Analyze the settlements and ground pressure at the surface due to the tunnel in the cases without and with the foundation structure in the vicinity.	Experimental
Castro et al.	2007	Study the “block caving” mining method, not the movements that occur on the surface of the land	Experimental large-scale 3D model
Trueman et al.	2008		
Lee & Bassett	2007	Simulate the deformation of the tunnel by changing its diameter, to investigate the behavior of existing foundations located near the tunnel	Experimental
Kikumoto et al.	2009		
Caudron	2007	Characterize the influence of soil-structure interaction during the formation of a sinkhole	Experimental and numerical
Deck and Anirudth	2010	To investigate the phenomenon of soil-structure interaction due to mine subsidence, taking into account the influence of length, rigidity of the structure, mechanical properties of the soil, and intensity of subsidence.	Numerical 2D model CESAR LCPC
Boramy Hor	2012	Simulate ground movements and their consequences on the surface.	Experimental/numerical 3D physical model
Al Heib et al.	2013	Understanding sinkhole consequences on masonry structures using a large small-scale physical modeling. The paper presents the main results of the small-scale physical model designed to study the consequences of subsidence on structures. Present the transfer of movements from the soil to the structure. The objective is to understand and then to predict the real behavior and the damage of structures on subsidence areas .	Experimental
Nghiem et al.	2014	Physical model for damage prediction in structures due to underground excavations: a small-scale physical model (1/40 scale factor on the dimensions) under normal gravity. It has been designed for developing and validating experimentally new methods of prediction of damages to masonry structures induced by subsidence (generally resulting from underground excavations of tunnels and mines)	Experimental
Keawsawasvong	2021	Limit analysis solutions for spherical cavities in sandy soils under overloading. An investigation on the stability of spherical cavities in sandy soils under overloading at the ground surface is carried out in this study. By using finite element limit analysis, a spherical cavity is numerically simulated under an axisymmetric condition, and the lower and upper bound solutions of the stability of spherical cavities can be obtained	Numerical

Continued **Table 1:** Summary of conducted research studie.

Author	Year	Objective	Type
Yongyao et al.	2023	A numerical simulation study on the evolutionary characteristics of the damage process of karst soil cavity under positive pressure effect	Numerical
Keba and Isobe	2024	Bearing capacity of a shallow foundation above the soil with a cavity based on a rigid plastic finite element method. Based on the rigid plastic finite element method (RPFEM), this study investigates the performance of the footing on the soil with a cavity. The RPFEM is used in plane strain conditions and necessitates only a few materials to predict the bearing capacity: the unit weight of the soil, the cohesion, the shear resistance angle, and the dilation angle	Numerical

Table 2: Empirical formulas for determining *i* (Dolzhenko, 2002).

Authors	Proposed expression	Soil type	Calculated *i* value
Atkinson & Potts. (1977)	i = 0.25(1.5C + D)	Dense sands with surcharge	3.65 m
Oteo & Sagaseta. (1982)	i = 0.525H + 0.42R	Granular soils	5.67 m
Dyer et al. (1986)	i = 0.29H	Loose to medium dense sand	2.60 m
Al Abram (1998)	i = 0.15H + 0.5D	Analogical soil	3.60 m

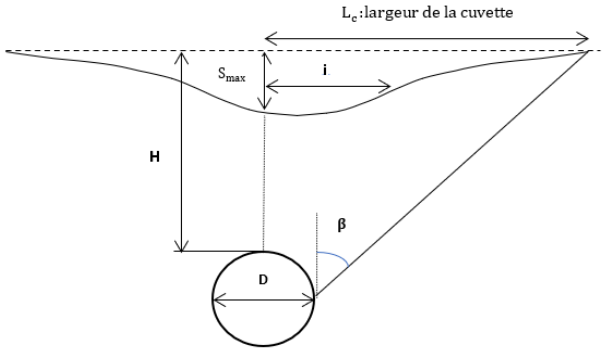


Figure 1: Schematic diagram of the empirical approach by Peck (1969).

$$\text{Horizontal displacement: } V(x) = S(x) \times \frac{x}{H} \quad (2)$$

The parameter *i*, representing the width of the collapse trough, can be approximated by various empirical relationships taking into account the diameter D, the cover C, and the nature of the soil (Table 2).

Caudron et al. (2006) demonstrated that with some modifications, the two expressions (eqs 1 and 2) can be used to predict surface displacements as long as the movement curves remain continuous. This is the case when the upper part of the lining is made of the granular material and the cavity is rectangular in shape. Mathematical treatment and integration of the value of the increment *i* depending on the soil type are presented in Table 2.

They manage to propose both equations related to vertical and horizontal displacements such that *i* is derived from the empirical formulas (Dolzhenko, 2002), where (i = 0.15H + 0.5D). The formulas then become as follows:

$$\text{Vertical displacement: } S(x) = \frac{0.667 V_{cavity}}{2.5i} \times e^{-x^2/2i^2} \quad (3)$$

$$\text{Horizontal displacement: } V(x) = S(x) \times \frac{(x/1m)}{(H/1m)^{\gamma}} \quad (4)$$

with an optimal value of γ equal to 0.87 and V_{cavity}=a×b (a and b the height and width of the cavity).

2 Case Study

The work of Caudron et al. (2007), which particularly focused on soil-structure interaction phenomena during the formation of a cavity near a surface frame, was used as a reference as it perfectly aligns with the concept of this research. The authors chose a real case (the Malakoff limestone quarry in the Paris region) involving a cavity of 10 meters wide and 2 meters high with a depth of 8 meters formed by 9 laminated soil layers (see Fig. 2) (Caudron, 2007; Caudron et al., 2006; Caudron et al., 2004).

The characteristics of the actual materials are detailed in Table 3.

Table 3: Geo-mechanical characteristics of different materials (Caudron, 2007).

Layer	Materials	E (MPa)	υ	$R_{traction}$ (MPa)	Cohesion (MPa)	φ (°)
8	Marls	70	0.25-0.30	0.30	0.80	28
2 and 5	Stones	100	0.25-0.30	0.30	0.80	29
6	Clay sand	130	0.25-0.30	0.20	1.2	30
3 and 9	Limestone	20	0.25-0.30	0.80	2.00	31
7	Stones	200	0.25-0.30	01	1.00	35
4	Marls	50	0.25-0.30	0.1	0.20	26
1	Stones	50	0.25-0.30	0.20	0.40	27

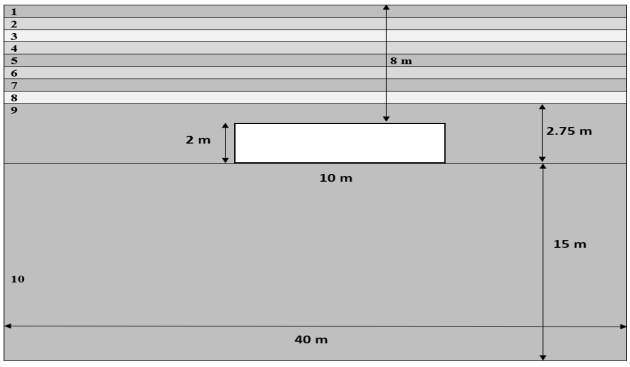


Figure 2: Real model of the cavity.

The main source of problems and complexity in designing a physical model lies in the importance of adhering to similarity rules with respect to the original phenomenon. Obviously, for a full-scale model, this is not limiting. The main limitation in this case comes from the cost and feasibility of tests.

This is why it is common to resort to reduced models, which present a number of advantages: speed, reproducibility, and the possibility of working until failure. However, to ensure that the phenomenon obtained in the reduced model exhibits behavior similar to that observed in full scale, it is necessary to ensure compliance with a number of rules. These are the laws of similarity, as presented by Dehousse and Arnould (1971) and by Bazant (2004). Since then, Garnier has specified their application to the field of geotechnics (Garnier, 2001a; Garnier, 2001b).

Each letter accompanied by an asterisk (*) represents the scale factor associated with the change in scale for the respective quantity. Table 4 provides the meanings of each quantity.

Caudron et al. (2006) extensively presented the small-scale physical model: design and limitations of the model. The first step in defining the small-scale physical model was the laws of similarity. The assumption is made that the thermal effect has no influence on the series of tests, which makes the problem somewhat simpler. Then, three scale factors must be determined in order to establish the entire relationship between the full-scale case study and the small-scale model. These scale factors concerned gravity, density, and length. The tests are carried out under normal gravity, so the corresponding scale factor is 1.

The analogous soil has a unit weight of 65 kN/m³, so the scale factor on density is 3. The final scale factor concerns

length. It was set at 1/40 in order to have a test bench with practical dimensions. From this point, all other scale factors can then be deduced from the laws of similarity and these three values. Therefore, it is not possible to adhere to all similarity rules, particularly those concerning stress states. The results of small-scale tests will then be qualitative rather than quantitative. The value 1/40 is chosen, which remains within the limits of the commonly accepted range of values for the Schneebeli material used (Ovesen, 1979) (see Table 5).

The experimental reduced model is simpler, represented at a scale of 1/40, with a soil mass of 1000 mm width for a covering height of 200 mm above the cavity (see Fig. 3).

The Schneebeli analog material, used to represent the soil, consists of a mixture of assemblies of steel rods with diameters of 3, 4, and 5 mm in precise proportions (see Fig. 4) (Schneebeli, 1956 ; Schneebeli, 1957). The lining consists of a cohesive bench with a thickness equivalent to 50 mm located at the top of the cavity. This is topped with a layer of pulverulent material equivalent to 150 mm in thickness. The cavity, with a height equivalent to 50 mm, is gradually created up to a maximum width corresponding to 250 mm in five steps (Caudron et al., 2004; Caudron et al., 2006; Caudron et al., 2007).

The structure used for the study of soil-structure interaction is of the steel beam-post type. The load

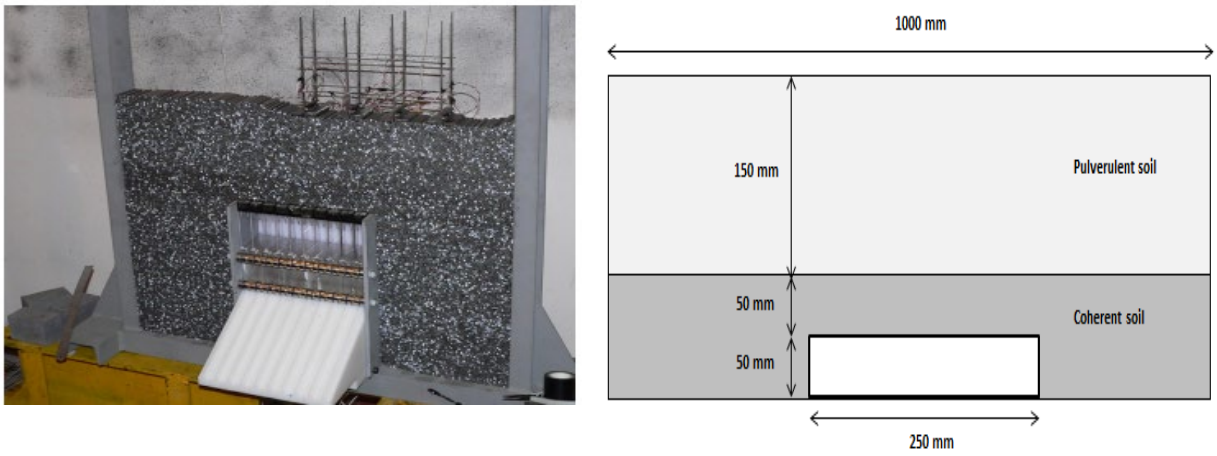


Figure 3: Experimental scale model.

Table 4: List of similarity laws.

Number	Similarity law	Meaning of scale factors
1	$x^*/L^*=1$	Equality of coordinates relative to length scale
2	$U^*/L^*=1$	Equality of displacements relative to length scale
3	$U_0^*/L^*=1$	Equality of displacements at origin relative to length scale
4	$g^*/\gamma^*=1$	Equality of acceleration scale to gravity scale
5	$E^*L^{*2}/F^*=1$	Conservation of the ratio of elasticity modulus scale by length squared to force scale
6	$\gamma^*t^{*2}/L^*=1$	Identity of acceleration and length scales as time cannot be altered
7	$P^*L^{*2}/F^*=1$	Conservation of the ratio of pressure scale times length squared to force scale
8	$(\sigma_0^*L^{*2})/F^*=1$	Conservation of the ratio of stress scales times length squared to force scale
9	$(\rho^*\gamma^*L^{3*})/F^*=1$	Conservation of the ratio between scales of quantities determining inertia force relative to force scale

Table 5: List of scale factors.

Symbol	Scale factor concerned	Dimension	Value
L*	Length of reference	L	1/40
x*	Coordinates	L	1/40
E*	Modulus of elasticity	$ML^{-1}t^{-2}$	3/40
ρ*	Density	ML^{-3}	3
g*	Acceleration of gravity	Lt^{-2}	1
F*	External punctual force	MLt^{-2}	3/64000
p*	Superficial force	$ML^{-1}t^{-2}$	3/40
U*	Displacement	L	1/40
σ*	Constraint	$ML^{-1}t^{-2}$	3/40
γ*	Inertia acceleration	Lt^{-2}	1

considered, uniformly distributed over the beam elements, corresponds to 10 kPa, comparable to permanent loads and service loads. The stiffness (ES and Eiz with E the Young's modulus, S the section, and Iz the moment of inertia) of the structural elements respects the scaling: the behavior obtained is purely elastic. The rules of similarity govern the relationship between a full-scale object and its scale model. In the context of a similarity that must account for the mechanical behavior of the object, a number of scale factors must be considered. Fig. 5 shows a schematic view of the full-size building as well as its scale model.

Table 6 shows the characteristics obtained from the predimensioning of the structure with the assumed data and the equivalent characteristics for the scale model with the similarity laws. However, the use of a coherent material is a prerequisite for representing the resistant bench needed to create the cavity.

All conducted characterization tests by researchers on the Schneebeli material show that its behavior is identical to that of dense sand (Dolzhenko, 2002; Kastner, 1982). Therefore, the material was modified by Caudron (2006) to represent a cohesive material.

Cohesion was achieved using an aqueous adhesive. Laboratory tests were conducted to determine the mechanical characteristics of the modified material, and

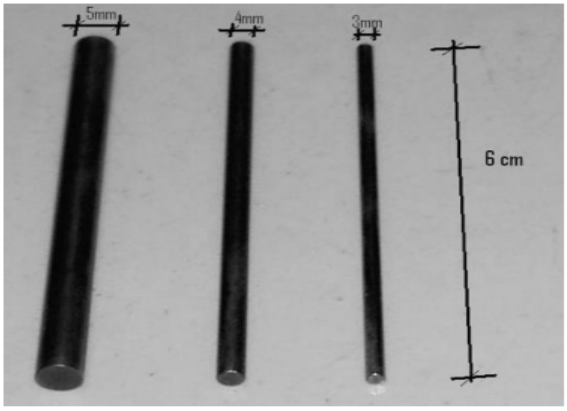
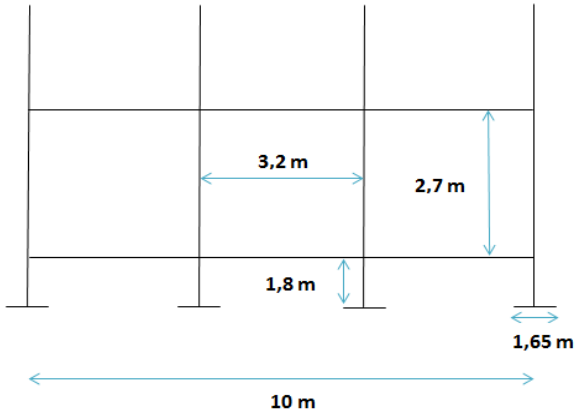


Figure 4: Overview of Schneebeli rolls.



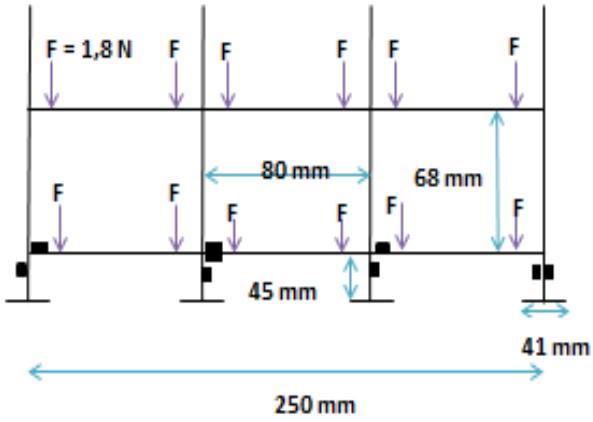


Figure 5: Real and scale model of the structure (Caudron et al, 2007).

the improvement concerns the friction angle, cohesion, and volumetric behavior from a pulverulent soil to a cohesive one. The biaxial tests, therefore, began with different concentrations of adhesive at C/2, C/4, and C/8 (C: glue concentration; C/2, C/4, and C/8: concentration

Table 6: Structure characteristics in real size and scale model.

Characteristics	Values	
	Real model	Scale model
Module (MPa)	33000	2475
Section (m^2)	0.04	25×10^{-6}
Inertia (m^4)	1.33×10^{-4}	52×10^{-12}
Loading (kPa)	10	0.75

Table 7: Geo-mechanical characteristics of scale model soils.

Characteristics	Unit	Pulverulent soil	Coherent soil
Young's modulus (E)	MPa	50–100	50–100
Friction angle (φ)	°	26	28–30
Cohesion (c)	KPa	≈ 0	≈ 200
Poisson's ratio (v)	/	0.3	0.3
Density (ρ)	kg/m^3	2200	2200

fractions), gradually diluting it until the desired behavior was obtained. Two concentrations of adhesive, those at C/4 and C/8, seem to allow obtaining a material that exhibits mechanical characteristics close to those desired. The modified material exhibits characteristics close to those desired, so they are more finely characterized in Table 7.

3 Numerical Modeling

The finite element method is employed to model the soil-structure interaction during the formation of a cavity. Once the model is established, a comparison between the numerical results and the experimental data from (Caudron, 2007), as well as those from the analytical method, will be performed. The modeling involves several successive and distinct steps, such as data input, definition of boundary conditions, meshing, calculation phases, simulation startup, and results analysis.

To model the structure, it is important to present all the data related to the different materials: building geometry, material properties (powdery and cohesive soil, air, column-beam structure, footings), load, cavity dimension, and depth. The schematic representation of the model is shown in Figure 6. It consists of a soil block with a height of 25 m and a width of 40 m. Comprising two superimposed soil layers, the upper layer is of powdery type with a height of 6 m overlying a cohesive soil layer

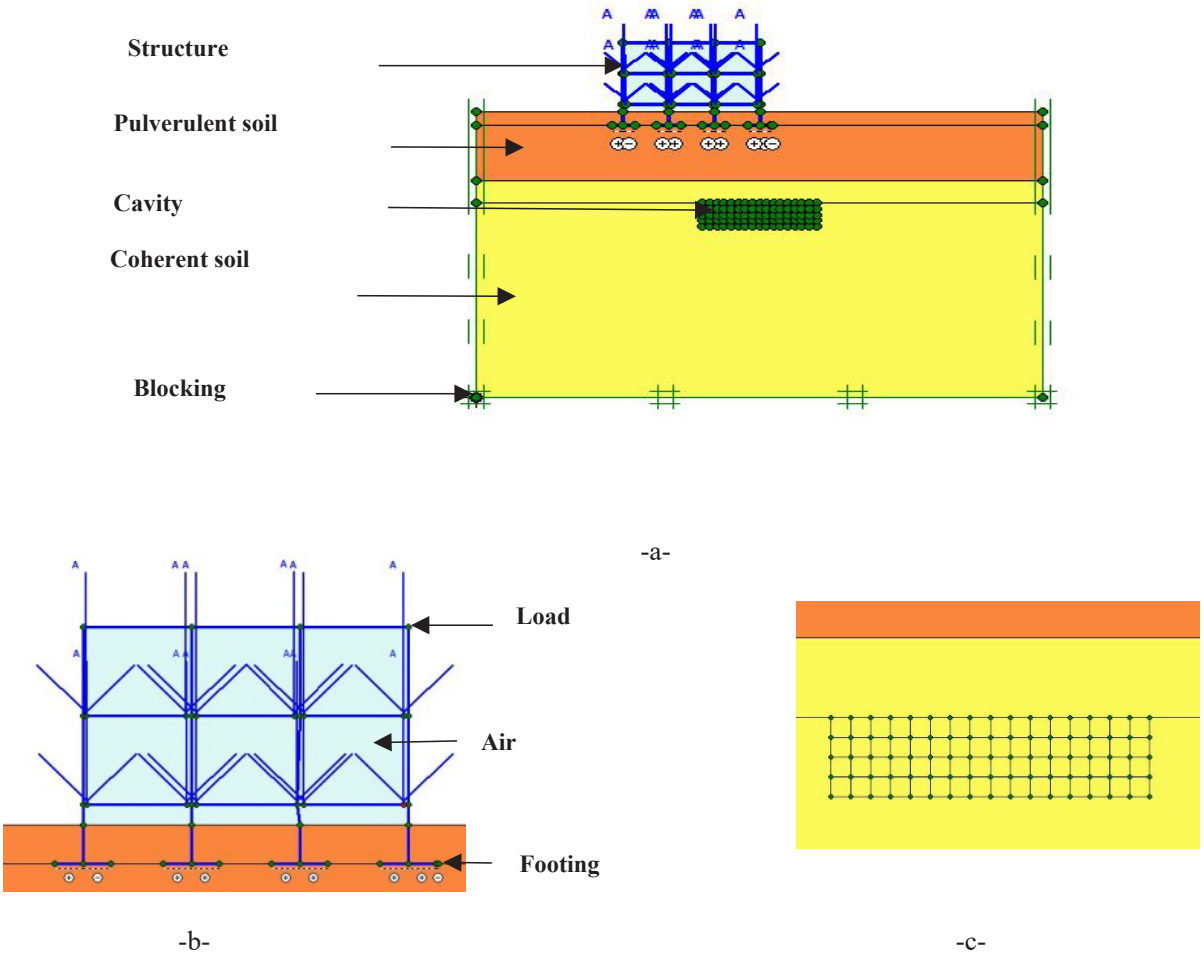


Figure 6: Model geometry: (a) global geometry, (b) structure, and (c) cavity diagramming.

with a height of 19 m. A two-level structure is embedded in the upper layer at a depth of 1.2 m. The lower layer encompasses a cavity with a height of 2 m and a length of 10 m in a rectangular shape.

Based on the values of the properties of the various materials used in the experimental study, the same values are incorporated into the material database of the numerical model. Tables 8 and 9, respectively, present the properties of the soils and structural elements. Among the problems encountered during the modeling is the representation of the rupture process and the simulation of the void present during the progression of the cavity. We chose the same properties for air to simulate the void existing between the structural elements. Air is represented as a material with low physical properties.

For the calculations, we assume that the interfaces between the different soil layers are perfectly adherent, implying continuity of vertical stresses and vertical displacements. Boundary conditions are ensured both by embedding the soil at the base and on the sides and by positioning the structure at a sufficiently distant distance from the edges to allow for good stress distribution in the soil.

The soil mass has been discretized entirely by 15-node triangular finite elements. The same type of elements has been adopted for meshing both the soil body and the structure to ensure correct assembly. The mesh consists entirely of 561 elements and 4631 nodes. Local mesh refinement has been performed in areas where strong gradients are likely to appear, i.e., around the cavity, to obtain a good estimation of stress and displacement fields (see Fig.7).

The reasoning process adopted for the calculation of such a model led us to establish 7 phases:

Phase 0: Initiation of stresses (K0 procedure) to determine initial effective stresses.

Phase 1: Excavation at the depth of the footings.

Phase 2: Installation of the structure.

This phase involves activating the structure (footings and framework) and backfilling to ensure the stability of

Table 8: Soil properties.

Parameters	Name	Unit	Pulverulent soil	Coherent soil	Air
Material model	Model	-	Mohr-Coulomb	Mohr-Coulomb	Mohr-Coulomb
Material type	Type	-	Drained	Drained	Drained
Soil unit weight above phreatic level	γ_{unsat}	kN/m³	17	20	5
Soil unit weight below phreatic level	γ_{sat}	kN/m³	19	22	5
Permeability in horizontal direction	k_x	m/day	1	0	1
Permeability in vertical direction	k_y	m/day	1	0	1
Young's modulus	E	kN/m²	100000	100000	5
Poisson's ratio	v	-	0.3	0.3	0.1
Cohesion	c	kN/m²	2	200	1
Friction angle	φ	°	26	26	5
Dilatancy angle	ψ	°	7	9	1
Strength reduction factor interne	R_{inter}	-	1	1	1

Table 9: Properties of structural elements.

Parameters	Name	Unit	Value
Type of behavior	Material type	-	Elastoplastic
Normal stiffness	EA	kN/m	132000
Flexural rigidity	EI	KNm²/m	4389
Equivalent thickness	d	m	0.632
Weight	w	KN/m/m	10
Poisson's ratio	*v*	-	0.35

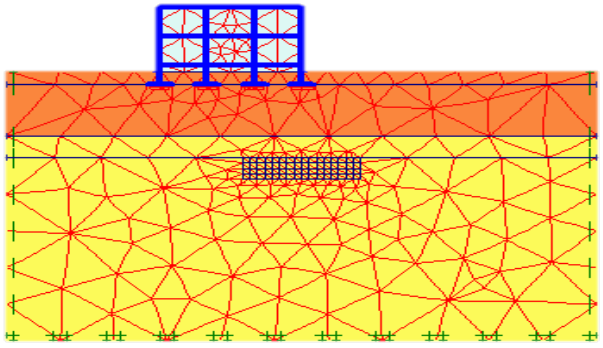


Figure 7: Model meshing.

the structure. At this stage, the soil is loaded only under its own weight.

Phase 3: Loading.

Phases 4, 5, 6, 7 represented in Figure 10 express the process of rupture numerically simulated according to the collapse mode of the cavity.

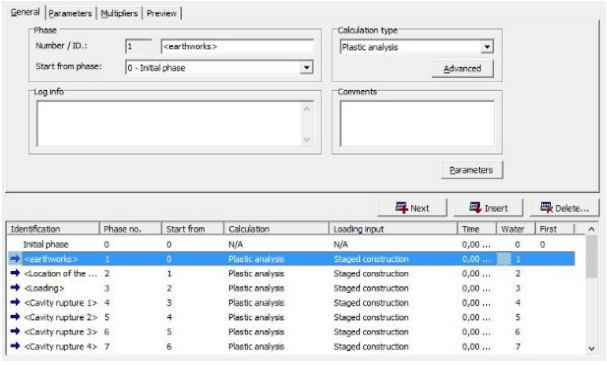
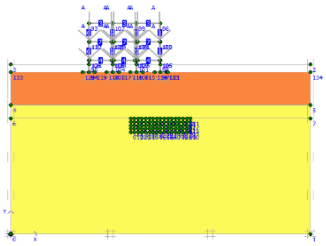


Figure 8: Calculation phases.

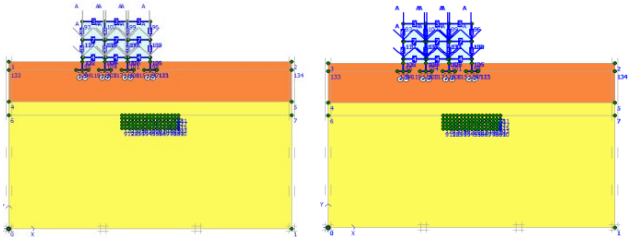
We triggered the rupture by initiating a thin layer of air void, which we then gradually extended until complete collapse.

After several attempts and corrections, the sequence of calculation phases has been established without interruption, and we have reached the phase of result exploitation (launch of calculations) as shown in Figure 11:

According to the experimental results (Fig. 12a), we observed that the rupture of the stiff bench occurs shortly after degradation. The latter fall into the cavity, and the soil reduced to powder on the surface follows their movement. The foundations of the structure are then evaluated, revealing some smaller voids in the fracture areas in the stiff bench and significant detachment of the right footing of the structure. Figure 12b presents the visualization of the last phase of the numerical model (total cavity

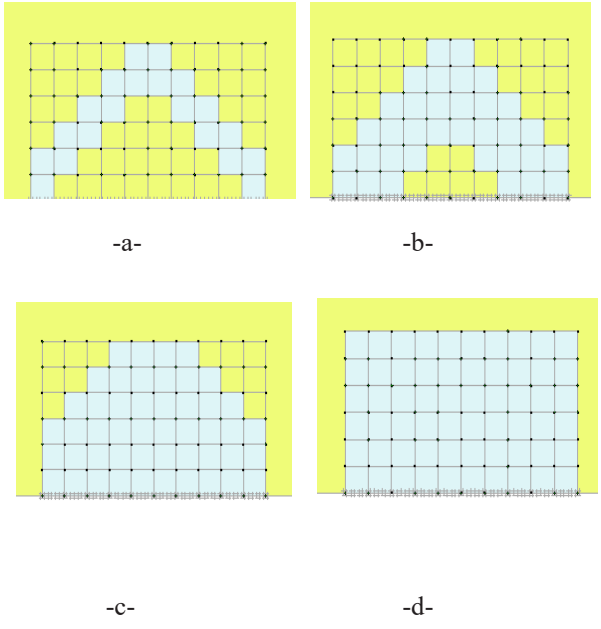


-a-



-b- -c-

Figure 9: Phases 1, 2, and 3: (a) Phase 1 (excavation), (b) Phase 2 (soil + structure), and (c) Phase 3 (loading).



-a- -b-

-c- -d-

Figure 10: Cavity rupture process.
(a) Phase 4 (initial cavity rupture)
(b) Phase 5 (2nd cavity rupture)
(c) Phase 6 (3rd cavity rupture)
(d) Phase 7 (total cavity rupture)

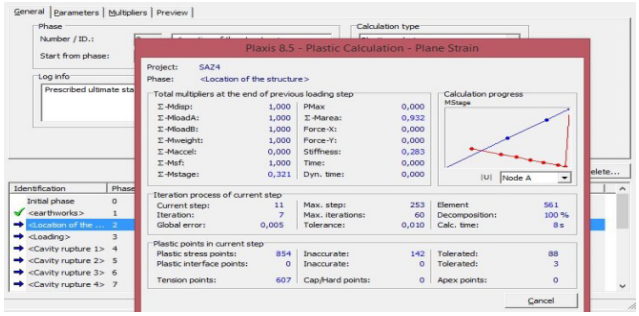


Figure 11: Calculation launch.

rupture). In this phase, the structure is tilted to the right, and consequently, the maximum displacement at footing 1 is recorded, as it is located at the cavity axis.

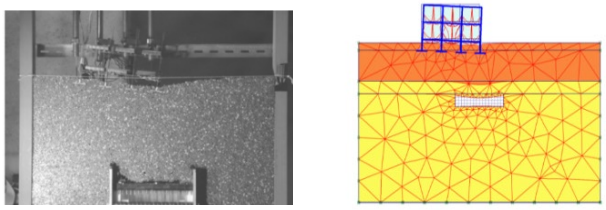
To demonstrate the validity of our model, we compared the results of vertical and horizontal collapses of different footings with the vertical and horizontal displacements at the surface of the cavity. The validation of the numerical model relies on comparing the results with those derived from experimental data and compared analytical results. Figures 13 and 14 display the results of the structure collapse comparison using analytical, numerical, and experimental methods. A good correlation is obtained between numerical and experimental results.

A slight deviation of 5 mm from the analytical results is observed. The maximum collapse occurs at footing 1, which is the most affected due to its positioning with the axis passing through the center of the cavity, unlike the other footings, which are slightly inclined.

The maximum displacement is observed on the right side of the structure, corresponding to the cavity axis (Position x = 20 m) (see Figure 13). Horizontal displacements are depicted in the graph (Figure 14), showing three curves with two types of positive and negative displacements. A significant influence of the structure is observed on the left side.

There is a good agreement between the curves of numerical, experimental, and analytical collapses, where the maximum value of numerical collapse is almost equal to that of experimental collapse (with a difference of a few millimeters). The maximum slope of collapse is located at the axis of the cavity. Gradients or breaks in the curve of the numerical method are attributed to the simulation of cavity rupture (see Figure 10c). In the numerical method, the cavity is subdivided into small squares, and the higher the number of squares, the more the gradient of the curve attenuates.

Figure 15 shows that the vertical displacements of the footings are identical for the experimental and numerical



a: Experimental b: Numerical

Figure 12: Final phase of rupture.

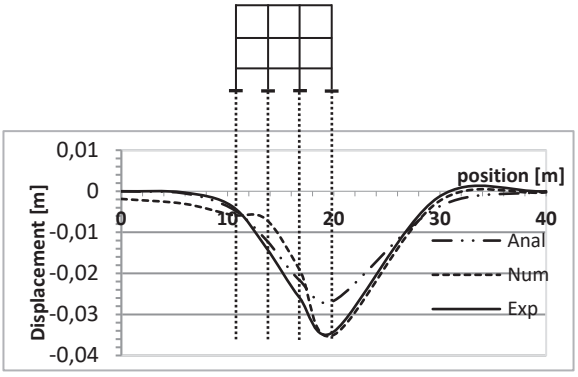


Figure 13: Vertical displacements (numerical, experimental, and analytical) of the footing.

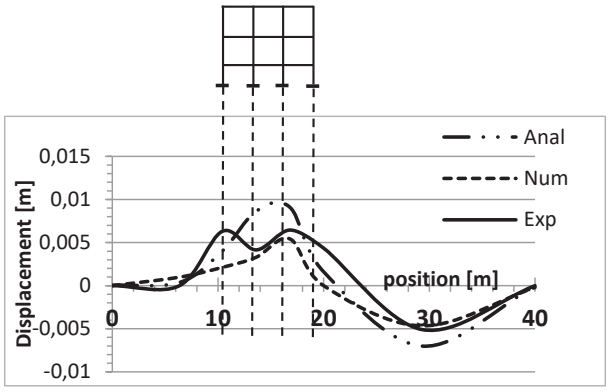
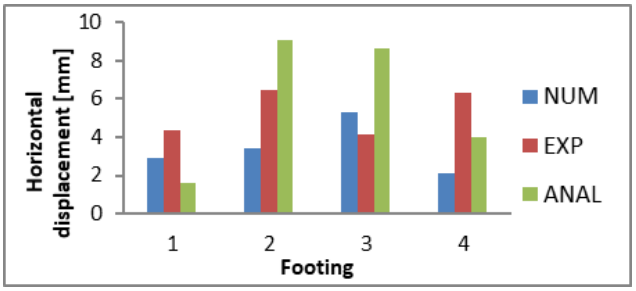


Figure 14: Horizontal displacements (numerical, experimental, and analytical) of the footings.

methods, although there is a slight difference for the analytical method (8.3 mm as the highest estimate for footing 4). It can also be observed that there is a slight difference in the horizontal displacements of the footings using the three numerical, experimental, and analytical methods (5.67 mm as the highest estimate for footing 2).



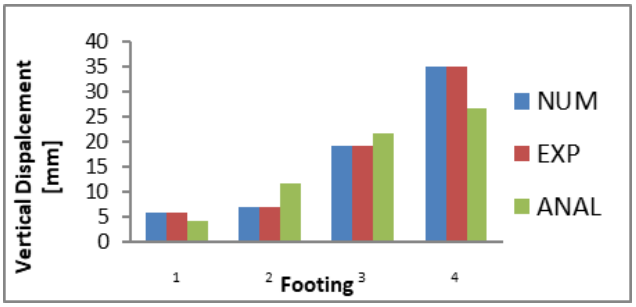


Figure 15: Differences in displacements of each footing among the three methods.

4 Analysis of Influencing Parameters

To study the gradual degradation of cavities and their impact on structure stability, a comparative method was employed to develop influential parameters such as volume, spacing, and depth of cavities. This approach will evaluate the effect of these parameters using variable ratios, including a ratio of b/a ranging from 0.5 to 3, a ratio of H/B varying from 0.5 to 3, and a ratio of L/B also ranging from 0.5 to 3. The dimensions B, H, a, b, and L are shown in Figure 12 (Djamel Saadi et al., 2020).

Figure 17 illustrates the behavior of the soil and the soil-structure interaction concerning the increase in cavity volume and structure instability. After analyzing the behavior of the footings, it is observed that those aligned with the cavity axis undergo more deformations than those away from this axis. Stress levels peak as the cavity volume increases. Vertical stresses are evident on the sides of the cavity, with a compression value of -450 kN/m².

The impact on the structure is negligible as the stress approaches zero, but the footings are exposed to stresses ranging from -150 kN/m² to -300 kN/m² depending on their position relative to the cavity.

The relative exploitation of results is presented in Fig. 18.

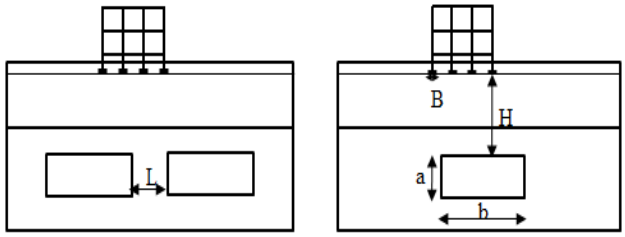


Figure 16: Models used in this study: (B) width of the footing, (H) depth of the cavity, (L) cavity spacing, (a) cavity height, and (b) cavity width.

From observing the curves of vertical and horizontal displacements (Fig. 18), it can be seen that each curve is symmetrical with respect to the cavity axis.

For the H/B ratio: The displacement value increases as the cavity depth decreases.

For the L/B ratio: The displacement value increases as the distance between the cavities decreases.

For the b/a ratio: We also notice that the displacement value increases with the increase in dimensions of cavity. This led us to search for an equation expressing the relationship between the cavity volume and the vertical and horizontal displacements that occur in the soil.

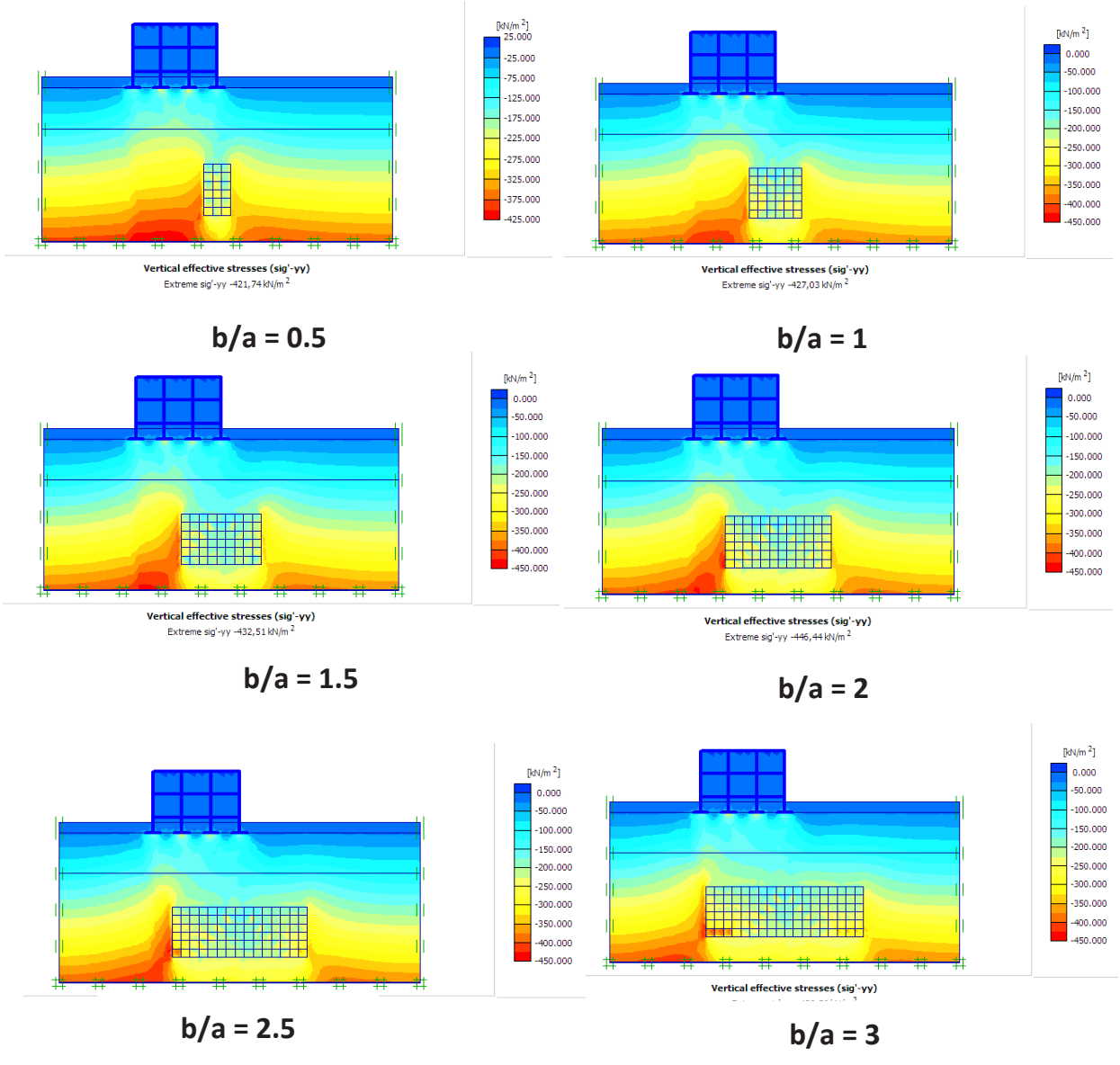


Figure 17: Stress in the yy plane.

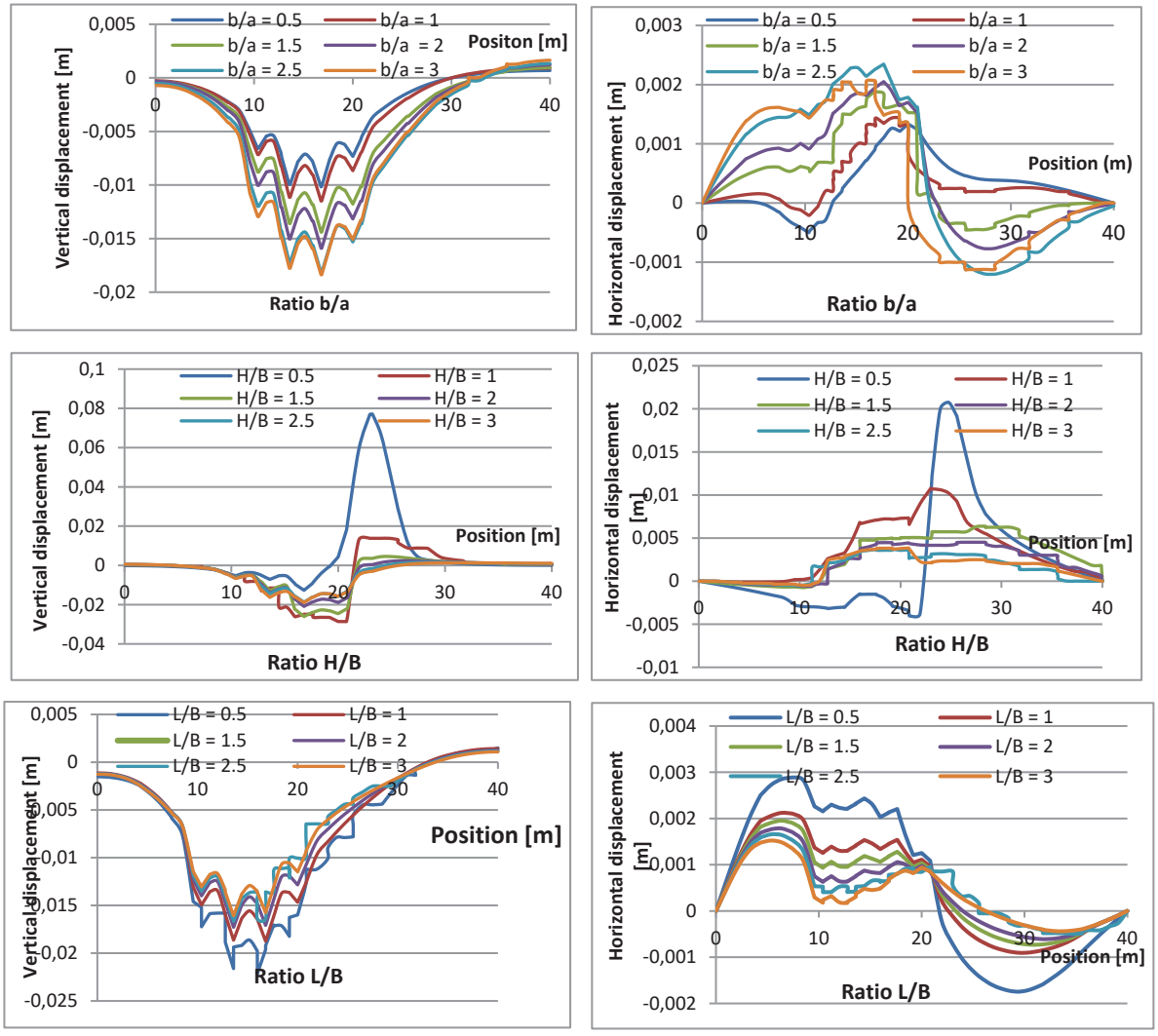


Figure 18: Vertical and horizontal displacements according to the three ratios.

The different profiles were analyzed based on the parameters a, b, H, B, and L, with trend lines plotted. The correlation coefficients R^2, ranging from 0.90 to 0.98, demonstrate a good fit of the data. The equations obtained from the curves in Figure 19 allow for accurate prediction of the horizontal or vertical collapse value based on the characteristics of the void beneath the structure (volume, depth, and spacing), as well as the initial displacement (without void), as illustrated in Equations 5 and 6.

$$U_y = U_{y_0}\left(0.347\frac{b}{a} + 0.9383 + 4.0803\frac{H}{B}^{-0.766} + 4.0803\frac{L}{B}^{-0.17}\right) \quad (5)$$

$$U_x = U_{x_0}\left(0.3525\frac{b}{a} + 0.9514 + 8.3075\frac{H}{B}^{-1.016} + 1.8262\frac{L}{B}^{-0.34}\right) \quad (6)$$

Equations 5 and 6 obtained are specific to the type of soil used in this study and provide an initial prediction. They can be used to anticipate the risks to which structures are exposed due to the rupture of cavities beneath the foundations.

According to Figure 20, we notice that the most influential ratio on the stability of the structure is the depth ratio of the cavity. This prompts us to focus our analysis on the significance of the void depth and its impact on structural instability. We also observe that the significance of volume, depth, and dimensions is more significant when the ratio lies between 0 and 2.5. Beyond a ratio of 2.5, all three parameters will have an equivalent impact.

5 Conclusion

In this study, we verified the validity of the numerical model by relying on both the results from an experimental

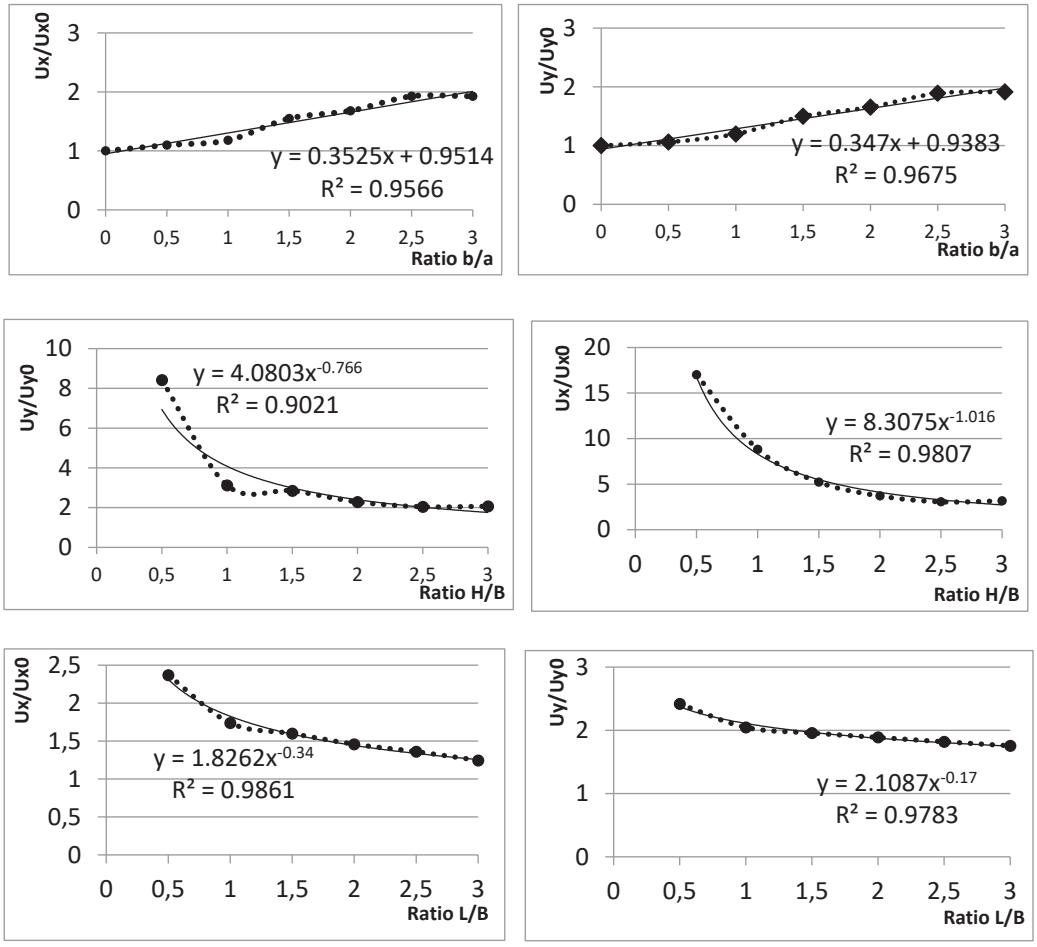


Figure 19: The variation in displacements under the three ratios.

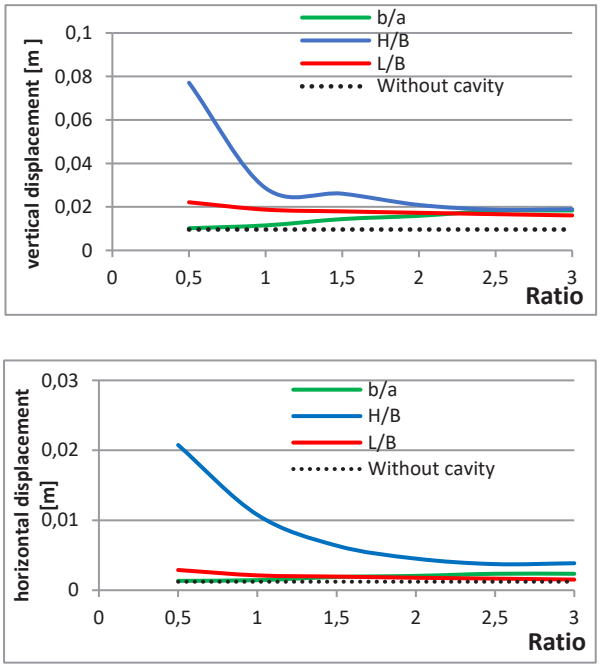


Figure 20: Displacement assembly according to the three ratios.

model conducted by one of the researchers and analytical laws. We furthered our investigation through a parametric study based on varying the ratio between the volume, depth, and distance between cavities.

- The obtained results are reliable, providing the developed model with a solid foundation for future case simulations.
- The stability of the footing above the cavity is influenced by several parameters related to it, notably its volume, depth, and the distance between two cavities.
- A correlation has been established between the footing displacement and the cavity properties (Equations 5 and 6). Although specific to the studied soil type, this relationship can be considered to assess the risk posed to structures due to the fracture of underlying cavities.

In this regard, this research was primarily proposed to analyze the cavity failure process leading to structural

instability due to the effect of differential displacement. This results in high stresses on load-bearing elements and the consequent appearance of cracks and fractures. Through the use of finite element methods, other parameters such as the position of the structure, anchoring of the footings above the void, and shape can be addressed to better understand the behavior of structures facing abrupt void collapses. These findings necessitate, in a subsequent study, proposing technical solutions to reduce potential disasters and analyzing their effectiveness in mitigating settlement and maintaining maximum structural stability until human intervention.

The next phase of this study will involve predicting the bearing capacity of the soil based on the three parameters, dimensions, depth, and spacing, and establishing their relationship with footing design principles. This risk management approach aims to prevent any significant damage and strengthen the margin of safety.

Symbols

H: height of the soil cover put at the end
D: tunnel diameter
x: distance to the center of the bowl
S(x): vertical settlement at the abscissa x
S_{max}: maximum surface settlement
i: distance to inflection point
Z_0: distance between surface and tunnel axis
E: Young's modulus
ν: Poisson coefficient
γ: volume weight of the soil
λ: rate of un-confinement
V(x): horizontal displacement at abscissa x
O: opening of the cavity
W: width of the cavity
U_x: horizontal displacement
U_y: vertical displacement
U_{x0}: horizontal displacement without cavity
U_{y0}: vertical displacement without cavity
a: height of the cavity
b: width of the cavity
B: width of the soles
L: length of the soles
n: porosity
C: cohesion
φ: friction angle
ψ: angle of expansion
C: initial glue concentration
$R_{Traction}$: tensile strength

References

[1] Aftes. The convergence confinement method. Recommendations, Tunnels, and underground structures, July 1982, pp. 98-105.

[2] Al Abram, I. Study on a two-dimensional reduced model of the displacement field induced by the digging of a tunnel at shallow depth. Interaction with existing works. PhD thesis, INSA Lyon 1998.

[3] Al Heib, M., Nghiem, H. L., and Emeriault, F." Understanding sinkhole consequences on masonry structures using large small-scale physical modeling." 7th international conference on Case Histories in Geotechnical Engineering The westin Chicago North Shore Wheeling Illiois 2013.

[4] Atkinson, J. and Potts, D. "Subsidence above shallow tunnels in soft ground." Journal of the Geotechnical Engineering Division,1977,103, 307– 325.

[5] Bazant, Z. Introduction to scale effects on structural strength. Paris: Hermes, 2004.

[6] Boramy Hor. Assessment and mitigation of the consequences of ground movements on buildings: experimental and numerical approaches. PhD thesis, INSA Lyon 2012.

[7] Boumalla, E. Definition and feasibility study of a reduced physical model for the study of the impact of subsidence and sinkholes on surface buildings Dissertation of the internship of the engineer of the Mines of Douai. Rapport de Master Recherche, Ecole des Mines de Douai, France 2005.

[8] Burd, H J., Houlsby, G T., Augarde, C E. and Liu G. Modelling tunnelling induced settlement of masonry buildings. Proc Inst Civil Eng: Geotech Eng, 2000, 143(1), 17–29.

[9] Caudron, M., Emeriault, F. and al Heib, M. Collapse of underground cavities and interaction with surface structures: experimental approach on a two-dimensional analogue model. National Geotechnical and Engineering Geology Days, Lille, France 2004.

[10] Caudron M., Emeriault F., Kastner R. & Al Heib M. 2006. Sinkhole and soil-structure interactions: Development of an experimental model. ICPMG, Hong-Kong, 04-06 Aug. 2006, pp 1261-1267.

[11] Caudron, M., Emeriault, F., al Heib, M.and R. Kastner. Numerical modelling of the soil structure interaction during sinkholes. National Geotechnical and Engineering Geology Days Lyon, France 2006.

[12] Caudron, M. Ground movements and deformations of a building following a sinkhole: experimental and numerical approach. INSA, Lyon, France 2007.

[13] Caudron, M. Experimental and numerical study of soil-structure interaction during the occurrence of a sinkhole. Thèse, INSA, Lyon, France 2007.

[14] Castro, R., Trueman, R. and Halim A. A study of isolated draw zones in block caving mines using a large 3D physical model. International journal of rock mechanics & mining sciences, 44, Julius Kruttshmitt Mineral Research Center, University of Queensland, Australia 2007.

[15] Deck O., Al Heib, M., Homand, F. & Wojtkowiak, F. Synthesis of methods for predicting the consequences of mining subsidence on buildings. Application to the case of the Lorraine iron basin. Mineral industry techniques, 2006, 29, 83-10.

[16] Deck, O., Anirudth, H. Numerical study of the soil-structure interaction within mining subsidence areas. Computers and Geotechnics, in press, 2010.
[17] Dehousse and Arnould. Scale models of structures in Civil Engineering. Paris: Dunod, 1971, 183.
[18] Djamel Saadi, Khelifa Abbeche, Rafik Boufarh. Model experiments to assess effect of cavities on bearing capacity of two interfering superficial foundations resting on granular soil, 2020.
[19] Dolzhenko, N. Experimental and numerical study of models, Two-dimensional reduction of tunneling. Development of a specific law of behavior. PhD thesis, National Institute of Applied Sciences, Lyon 2002.
[20] Dyer, M., Hutchinson, M. and Evans, N. Geotechnicals aspects of underground construction in soft ground, chapter Sudden valley sewer : a case history, 671–676. Rotterdam 1996 : A.A. Balkema.
[21] Dyne, L. The prediction and occurrence of chimney subsidence in southwestern Pennsylvania. Master of Science in mining and minerals engineering, Virginia Polytechnic Institute and State University 1998.
[22] Keba Lukueta E ., Isobe K. Bearing Capacity of a Shallow Foundation above the Soil with a Cavity Based on Rigid Plastic Finite Element Method. *Applied Sciences.* 2024; 14(5):1975. https://doi.org/10.3390/app14051975.
[23] Garnier, J. Physical models in geotechnics. Evolution of experimental techniques and fields of application. French Journal of Geotechnics, 2001a, 97, 3–29.
[24] Garnier, J. Physical models in geotechnics. Method validation and application examples. Revue Française de Géotechnique, 2001b, 98, 5–28.
[25] Kastner, R. Deep Excavations in Urban Sites. PhD thesis, INSA, Lyon 1982.
[26] Keawsawasvong, S. Limit analysis solutions for spherical cavities in sandy soils under overloading. Innov. Infrastruct. Solut. 6, 33 (2021). https://doi.org/10.1007/s41062-020-00398-5
[27] Kikumoto, M., Shanin, H. M., Nakai, T., Nagata, M. and Toda, K. Influences of tunnel excavation on the neighboring group-pile foundation. Proc. of 54th Geotechnical Engineering Symposium, 2009, 54, 355-362.
[28] Kratzsch, H. Mining subsidence Engineering. Spring-Verlag, Berlin/Heideilberg, New York 1983.
[29] Laefer, D. F. Predicting and assessment of ground movement and building damage induced by adjacent excavation, PhD thesis, The University of Illinois, Urbana, Ill. (2001).
[30] Lake, L., Rankin, W,and Hawley, J. Prediction and effects of ground movements caused by tunneling in the soft ground beneath urban areas. Construction Industry Research and Information Association, London 1992, UK: CIRIA Project Report 30.
[31] Lee, Y., Bassett, R. Influence zones for 2D pile-soil-tunnelling interaction based on model test and numerical analysis. Tunneling and underground space technology 22 (2007) 325-342.
[32] Mahamma, F. Behaviour of structures built on the surface during subsidence of old careers. DEA thesis, INSA de Lyon 2002.
[33] Nakai, T., Xu, L. and Yamazaki, H. 3D and 2D model tests and numerical analyses of settlements and earth pressures due to tunnel excavation. Soils and Foundations, (1997), 37, 31-42.
[34] Nghiem, H. L., Heib, M. A., & Emeriault, F.. Physical model for damage prediction in structures due to underground excavations. International conference on geotechnical engineering (Geoshanghai 2014), May 2014, Shanghai, China. pp.155-164. ffineris-01863823.
[35] Oteo, C. and Sagaseta, C. "Prediction of settlements due to underground openings." International Symposium on Numerical Models in Geomechanics, Ghent, Belgium,1982, 653–659.
[36] Peck, R. B. Deep excavation and tunneling in soft ground. Proceeding of the 7th International Conference of Soil Mechanics, Mexico: State-of-the-Art, 1969, Vol.3, pp.225-290.
[37] Schneebeli, G. "A mechanics for cohesionless soils" Minutes of the Academy of Sciences, Paris: 1956, Tome 243, pp. 2647-2673.
[38] Schneebeli, G. A mechanical analogy for the study of the stability of two-dimensional earth structures. Proceedings of the 4th International Conference on Soil Mechanics & Foundation Engineering (I.C.S.M.F.E.). London 1957.
[39] Shahin, H., Nakai, T., Hinokio, M., Kurimoto, T. and Sada, T. Influence of surface loads and construction sequence on ground response due to tunneling. Soils and Foundations, 2004, 44, 71-84.
[40] Sung, E., Shahin, H., Nakai, T., Hinokio, M. & Makoto, Y. 2006. Ground behavior due to tunnel excavation with existing foundation. Soils & Foundations, 2006, 2:189-207.
[41] Yongyao Wei and al. A numerical simulation study on the evolutionary characteristics of the damage process of karst soil cavity under positive pressure effect. Geohazard Mechanics. Volume 1, Issue 4, 2023, Pages 288-296, ISSN 2949-7418, https://doi.org/10.1016/j.ghm.2023.10.002.